An Investigation of Material Properties for a Selection of Chalcogenide Glasses for Precision Glass Molding.

William V. Moreshead, Jacklyn Novak, Alan Symmons
LightPath Technologies, Inc., 2603 Challenger Tech Ct, Ste 100, Orlando, FL, USA 32826

ABSTRACT

The growing demand for lower cost infrared sensors and cameras has focused attention on the need for low cost optics for the long wave and mid-wave infrared region. The combination of chalcogenide glasses and Precision Glass Molding (PGM) is the enabling technology for low cost infrared optics. The lack of detailed material properties data has limited its acceptance in the commercial market, but increased demand and recent cost reductions in infrared sensors has focused additional attention onto these materials as a cost driver for infrared systems.

This investigation reviews the material performance and repeatability for a number of different chalcogenide glasses. Material properties including composition, glass transition temperature (T_g), coefficient of thermal expansion (CTE), index of refraction, transmission and change in index over temperature (dn/dT) are explored. Specific attention is given toward glasses that achieve high yields during precision glass molding and are candidates for commercial success.

Keywords: Precision glass molding, chalcogenide

1. INTRODUCTION

Over the past ten years, the prices for thermal imaging sensors have decreased dramatically. The resulting cost savings has significantly increased the quantities of thermal imagers sold. Optics manufacturers are looking for high volume, low cost methods for producing infrared optical systems. The technological roadmap for infrared optical systems is following the same path that visible camera systems have followed in the recent past; from large SLR type cameras to small handheld cameras and finally to cell phone camera systems. The enabling technology for the visible region was molding of optical lenses. The expectation is that precision glass molding of chalcogenides will enable low cost optics in the infrared.

Until the past few decades, the only infrared optical materials available were crystals or salts that required expensive processing techniques such as single point diamond turning. Newer materials such as chalcogenide glasses were invented to allow the molding of infrared optics. Figure 1 shows an assortment of IR lenses molded from chalcogenide glass. Until recently, the availability and costs of chalcogenide glasses prevented widespread acceptance.

Figure 1 – Molded chalcogenide glass lenses

Electro-Optical and Infrared Systems: Technology and Applications IX, edited by David A. Huckridge, Reinhard R. Ebert,
Proc. of SPIE Vol. 8541, 854102 · © 2012 SPIE · CCC code: 0277-786/12/$18 · doi: 10.1117/12.970433

Chalcogenide materials were found to have several material properties that are advantageous to optical and opto-mechanical designers. These properties include such factors as moldability, better transmission than germanium at temperatures above 60-80°C [1] a combination of CTE and dn/dT that reduces focal shift as a function of temperature.

Optical quality germanium exists as a crystal and the two traditional methods for processing germanium are grinding and polishing for spherical surfaces and single point diamond turning (SPDT) for aspheric surfaces. Infrared optical systems that use only spherical lens elements tend to be very large, bulky and expensive. Aspheric elements allow for a more compact design, but may drastically increase the cost of the lens assembly. Chalcogenide glass was designed as an amorphous material and can also be ground & polished, diamond turned, or molded. Precision Glass Molding (PGM) is the most cost-effective method for producing high volumes of high performance infrared optics. [2]

Germanium is a well established material and it is well known that the dn/dT and CTE values cause large shifts in the focal plane of an imaging system as the external temperature changes. This is critical for thermal imaging systems as they are commonly used in applications that operate over a large ambient temperature range such as firefighting cameras, automotive night vision enhancement, or thermal sights for guns, artillery, and missiles. Optical systems typically have complex mechanisms for adjusting the positions of the lenses in order to maintain focus on the detector focal plane. The benefit to chalcogenides is that they require smaller ranges of motion to maintain focus which allows for passive mechanisms to athermalize the lens assembly.

As optical and opto-mechanical designers become more comfortable with chalcogenide glass as an attractive material alternative to germanium and zinc selenide for infrared optics, the questions of availability, production quality and uniformity become important to address.

To accurately model the behavior of an opto-mechanical system, accurate material property data and manufacturing tolerance information is essential for the optical and mechanical designers. Optical engineers need reliable transmission and index of refraction data over a range of temperatures to design high performance optics. Opto-mechanical engineers rely on CTE data in order to ensure systems don't fail under thermal loads and that lens assemblies maintain the correct focal distances.

In the case of PGM, the process requires detailed understanding of the glass composition, the softening point of the glass, and the thermal characteristics of the glass. All of these values drive the design and material selection of the molding tools and the optimization of the molding process parameters. The PGM process for chalcogenide glass is described in detail in previous publications [2-3].

Currently, chalcogenide glass is commercially manufactured by a handful of vendors. Each vendor has a selection of chalcogenide compositions. These compositions have different trade names, but can be reported to be the same at the first order. However, concerns remain that they may differ in minor impurities that affect the optical and mechanical properties of the material itself. An image of a typical boule of chalcogenide glass from a manufacturer is shown in Figure 2.

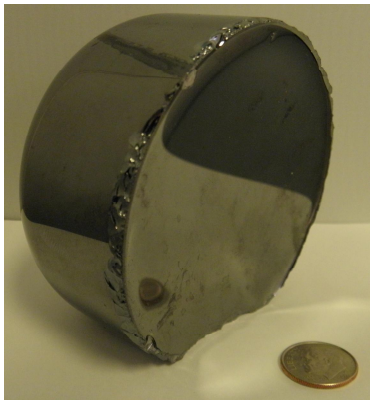

Figure 2 – 100mm boule of chalcogenide glass

The purpose of this paper is to examine a cross section of commercially available chalcogenide glasses, measure the nominal values for the critical optical and mechanical properties for each glass on a batch to batch and manufacturer to manufacturer basis.

2. EXPERIMENT

Several experimental techniques were used in order to characterize the optical, thermal, physical, and mechanical properties of several glass samples. Glass from three manufacturers were characterized. Two manufacturers make $Ge_{28}Sb_{12}Se_{60}$ and will be referred to as $Ge_{28}Sb_{12}Se_{60}$-A and $Ge_{28}Sb_{12}Se_{60}$-B, while the third manufacturer makes $Ge_{20}Sb_{15}Se_{65}$ and will be referred to by that composition. To explore repeatability, three different batches, or boules, of each glass were characterized from $Ge_{28}Sb_{12}Se_{60}$-B and $Ge_{20}Sb_{15}Se_{65}$. The purpose of these experiments is to evaluate various commercial manufacturers of chalcogenide glass. The properties of $Ge_{28}Sb_{12}Se_{60}$-A and $Ge_{28}Sb_{12}Se_{60}$-B were compared to published data on Schott/Vitron's IG5 and Amorphous Materials' AMTIR-3 while the properties of the $Ge_{20}Sb_{15}Se_{65}$ glass boules were compared to Umicore's GASIR2. AMTIR-3 is no longer produced, so the data cannot be verified but is used as a historical reference.

2.1 Particle-Induced X-Ray Emissions (PIXE)

The material samples were tested for their elemental make-up using proton-induced or particle-induced X-ray emission (PIXE) analysis. The PIXE technique is based on the principle that when a substance is exposed to an ion beam, it gives off electro-magnetic radiation specific to each element within the sample. The individual wavelengths measured identify the unique elements within the sample. Table 1 below shows the energies of the major X-ray emissions used to quantify the amount of elements commonly used in chalcogenide glasses.

Table 1: X-ray emission energies used to quantify chalcogenide glass elements in PIXE analysis

Element Name	X-Ray Energy (keV)	X-Ray Wavelength (nm)
Antimony	3.604	344.02
Germanium	9.887	125.40
Arsenic	10.544	117.59
Selenium	11.222	110.48

For the purposes of this experiment, bulk samples in the form of discs with fine-ground surfaces were used for PIXE analysis. While the accuracy of the absolute values obtained from this measurement technique can be questioned based on the fact that the numbers can change depending on how the data is treated, comparisons can be made between different samples and conclusions can be drawn about variation from boule to boule and manufacturer to manufacturer.

2.2 Differential Scanning Calorimetry (DSC)

The glass transition temperature (T_g), of the samples was determined using a TA Instruments Q1000 V9.9 DSC. Two hermetically sealed aluminum pans are placed in the DSC, one containing a 15-20 mg powdered glass sample and one empty reference pan. The two pans are heated at a rate of 10°C/min and the difference in heat flow between the reference and the sample is tracked. The heat capacity of the glass changes when it reaches its T_g, requiring more heat to flow to the sample pan than the reference pan in order to maintain them at the same temperature. This shows up as a step in the baseline of the DSC curve. The onset of this change in heat capacity is commonly reported as the T_g, and the procedure for determining the T_g from the curve can be found in [4].

DSC has some advantages over dilatometry for determination of the T_g of a glass, including easier sample preparation, less time to make the measurement, and the possibility to directly determine other properties such as heat capacity above and below the T_g.

2.3 Dilatometry

The samples were tested for their CTE and dilatometric softening point (T_d) using a NETZSCH DIL 402 C dilatometer. A sample in the form of a rod is placed in the dilatometer with a push rod touching one end. As the material is heated, it expands and moves the push rod. The change in the length of the sample rod, ΔL, is normalized to the initial length, L_0, and plotted vs. temperature. The slope of this line gives the CTE of the material. The CTE changes when the glass

reaches its dilatometric glass transition temperature ($T_{g(dil)}$), not to be confused with the T_g. A sample dilatometry curve is shown in Figure 3 below and the $T_{g(dil)}$ and T_d are indicated. The shape of the curve and the values of CTE, $T_{g(dil)}$, and T_d are dependent on the heating rate used in the experiment, which was 3°C/min for these samples.

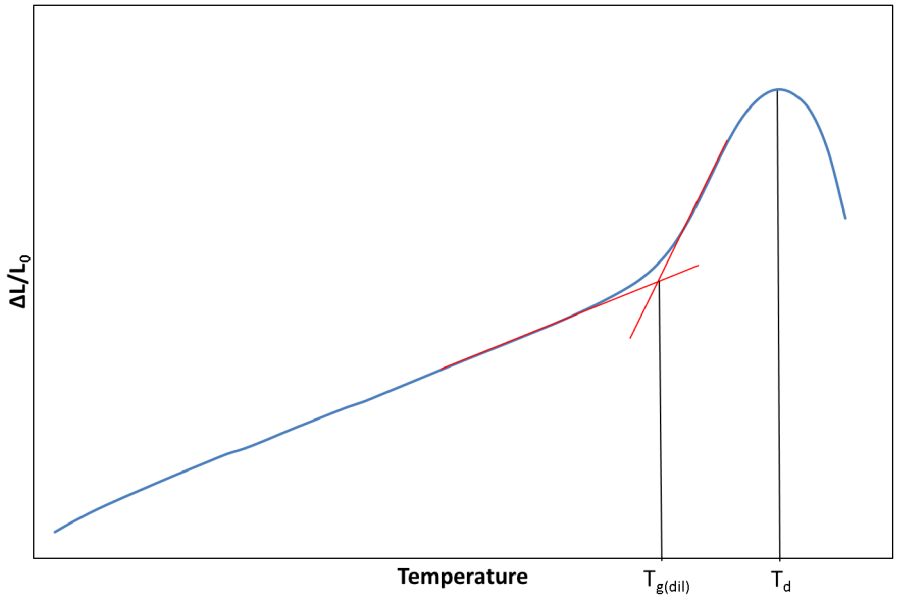

Figure 3 – Example dilatometer curve.

The rods used for dilatometry were at least 2" in length in order to minimize error, and had a rectangular cross section with each side being 7-10 mm, as seen in Figure 4.

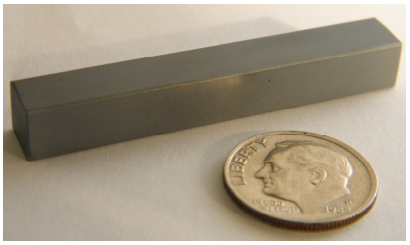

Figure 4 – Photo of dilatometry sample rod

2.4 Density

The density of a material is defined as its mass per unit volume. This can be determined through direct measurement of the mass and volume, although volume measurements are prone to error, especially for complex geometries. The method used for the purposes of these experiments was using Archimedes' principle to determine the volume of a sample by the amount of liquid it displaces. The weight of the sample is measured in air as well as in a liquid of known density and then the following equation is applied:

$$\rho = \frac{m_{air}\rho_L}{(m_{air} - m_{sub})}$$

In this equation, ρ is the density of the sample, ρ_L is the density of the liquid, m_{air} is the mass of the sample in air, and m_{sub} is the apparent mass of the submerged sample. The liquid used for these measurements was diethyl phthalate.

2.5 Hardness

For hardness measurements, a force is applied using an indenter with a known geometry. For these experiments, a P-macro/nano mechanical tester based on the ASTM E2546 and ISO 14577 standards for instrumented indentation was

used. A Berkovich diamond indenter was used. The displacement of the indenter relative to the sample surface is recorded throughout the measurement. A load/displacement curve is obtained and the hardness can be calculated. For each sample, 5 indentations were made and the average microhardness was calculated. The Young's Modulus of the sample can also be calculated from the data by finding the slope of the linear portion of the stress-strain curve. For all samples, the maximum force was 20mN, the loading rate was 40mN/min, the unloading rate was 40mN/min, and the creep was 20s.

2.6 Fourier Transform Infrared Spectroscopy (FTIR)

Transmission FTIR was performed on samples of approximately 5 mm thickness with parallel optically polished surfaces using a PerkinElmer Spectrum GX FTIR spectrometer. Measurements were made at room temperature under a nitrogen atmosphere and a background spectrum was collected before each sample spectrum. FTIR spectra were used to determine the spectral range in which the samples are transparent, as well as the average transmission in this range. The spectra can also be used to identify impurities, such as oxides and water, based on the location of their characteristic absorption bands.

2.7 Refractive Index

The refractive index of each glass boule was measured via a modified minimum deviation technique at M^3 Measurement Systems, Inc. This technique is accurate to the 5^{th} decimal place at room temperature. Samples must be in the form of a small prism with a specific geometry. Without the correct geometry and sufficiently flat surfaces, the accuracy of the measurement is decreased. For the prism sample, the index was measured at 20°C in air at 1.5, 2, 3, 5, 8, 10, 12, and 14 µm. Then the index was measured at each of these wavelengths under vacuum at temperatures ranging from -40 to 80°C in order to determine the change in index with temperature (dn/dT) at each wavelength.

3. RESULTS & DISCUSSION

3.1 Particle-Induced X-Ray Emissions (PIXE)

PIXE analysis was used to study compositional variations between different boules of glass. Various trace elements were found in these glasses but only the ratio between germanium, antimony, and selenium was studied in detail. The trace elements present were not the same for all of the samples. The results for $Ge_{28}Sb_{12}Se_{60}$-A and the three $Ge_{28}Sb_{12}Se_{60}$-B boules are shown in Figure 5 below and compared to the theoretical composition. Error bars are within the size of the data points.

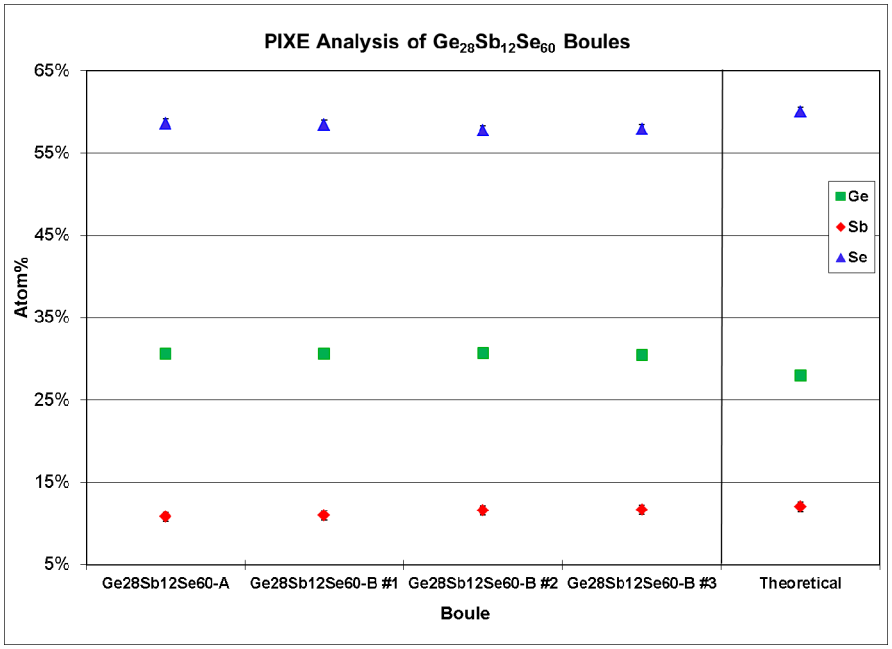

Figure 5 – Comparison of the composition of $Ge_{28}Sb_{12}Se_{60}$-A and $Ge_{28}Sb_{12}Se_{60}$-B glasses

As can be seen in the figure, the antimony content is close to the theoretical value for all 4 boules. However, all of the glasses had an excess of germanium and a deficiency in selenium content. It is interesting to note that the compositions of the glasses from the two different manufacturers were very similar even while differing from the theoretical composition. There is no significant difference in composition between the four boules of glass.

The results of the PIXE analysis of the composition of three $Ge_{20}Sb_{15}Se_{65}$ glass boules are shown below in Figure 6 and compared to the theoretical composition. Error bars are within the size of the data points.

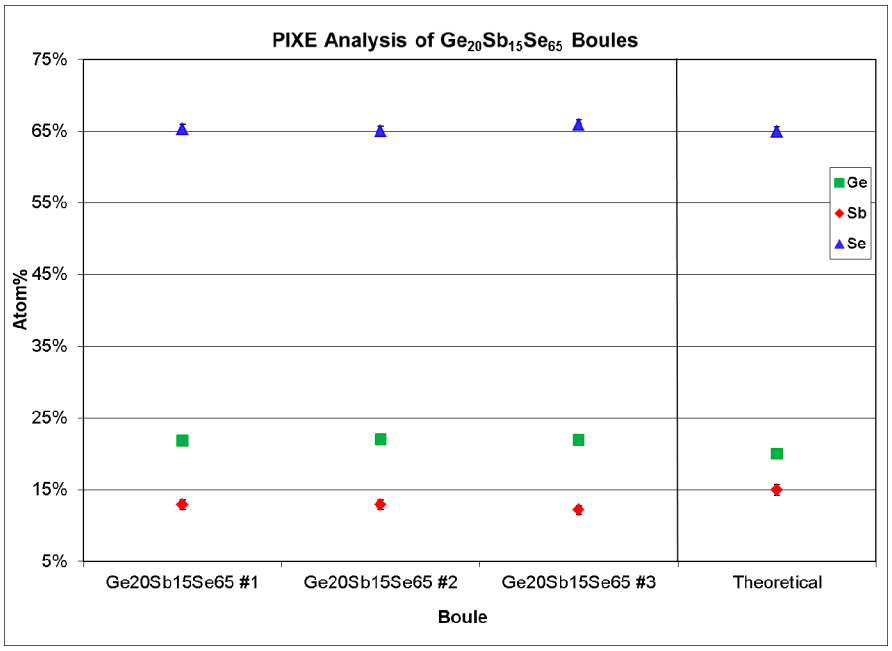

Figure 6 – Comparison of the composition of 3 $Ge_{20}Sb_{15}Se_{65}$ boules.

In this glass, the excess of germanium is seen just as in the previous composition. However, there is a lack of antimony while the selenium content is very close to the theoretical value. There is no significant difference in composition between the three boules.

3.2 Differential Scanning Calorimetry (DSC)

DSC was used to determine the T_g of each boule of glass. The T_g was calculated by finding the intersection of lines tangent to the DSC curve before and after the onset of the glass transition. This was done using the "onset point" function in TA Instruments' Universal Analysis software. An example is shown below in Figure 7.

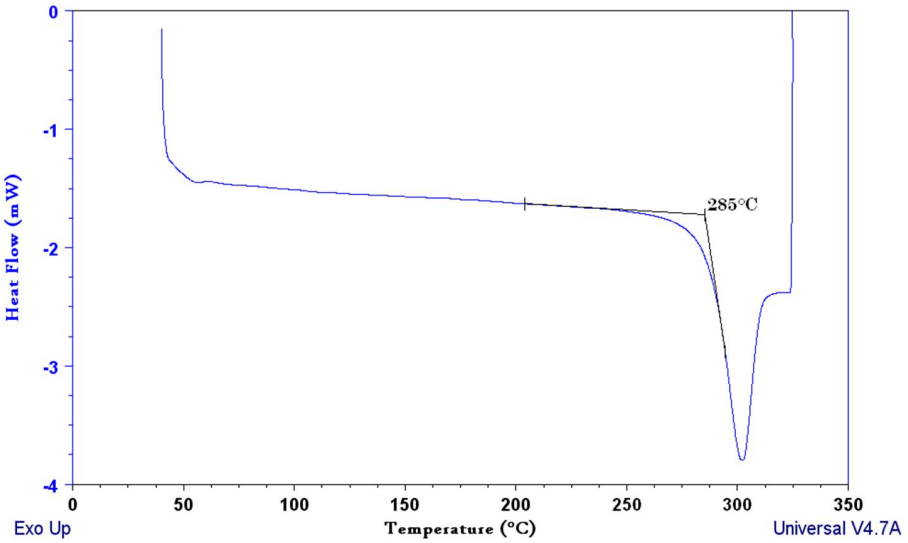

Figure 7 – Determination of the T_g from the DSC curve of $Ge_{28}Sb_{12}Se_{60}$-B boule #3.

This was repeated for each sample and the values were compared to published values of equivalent glasses. The results are plotted below in Figure 8.

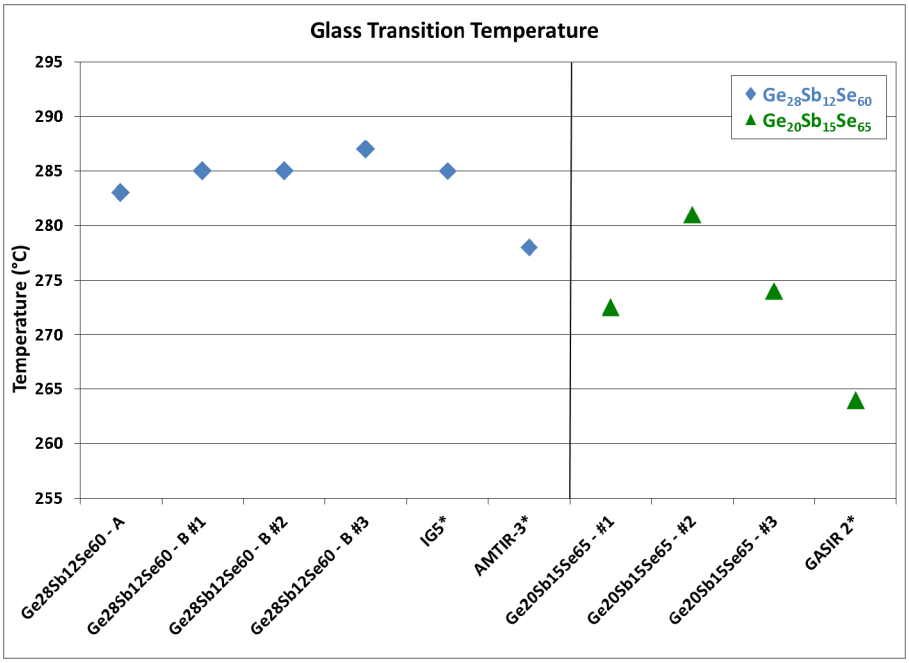

Figure 8 – Comparison of T_g values of various glass boules. *Indicates values from published data sheets.

The T_g's of $Ge_{28}Sb_{12}Se_{60}$-A and the $Ge_{28}Sb_{12}Se_{60}$-B glass boules are all very similar, approximately 285°C, which is also the published value for Schott's IG5 glass. The published value of the T_g of AMTIR-3, made by Amorphous Materials, is somewhat lower, 278°C. This variation could arise from several things, including differences in composition, glass melting procedures, experimental parameters, and determination of the T_g from the DSC curve. The main thing to take from this information is that there is no significant variation in the T_g between $Ge_{28}Sb_{12}Se_{60}$-B glass batches.

The T_g data for $Ge_{20}Sb_{15}Se_{65}$ is also plotted in the figure and there is much more variation than the $Ge_{28}Sb_{12}Se_{60}$-B boules. This could indicate inconsistencies in the process, especially during the quenching and annealing stages since there were no significant compositional variations seen. Another important note is that all of the T_g values for

$Ge_{20}Sb_{15}Se_{65}$ are at least 8°C above the reported value for the equivalent GASIR 2 glass. This could be for the same reasons listed previously.

For the purposes of PGM, the temperatures of the various stages of the molding process are chosen based on the thermal properties of the material. It is possible that variations in the T_g from batch to batch, such as seen in the $Ge_{20}Sb_{15}Se_{65}$ boules, could affect the molding process.

3.3 Dilatometry

Dilatometry was used to determine the CTE, $T_{g(dil)}$, and T_d of the samples. This test was performed on sample rods from the following glass boules: $Ge_{28}Sb_{12}Se_{60}$-A, $Ge_{28}Sb_{12}Se_{60}$-B #1, and $Ge_{20}Sb_{15}Se_{65}$ #1. The resulting curves are plotted in Figure 9.

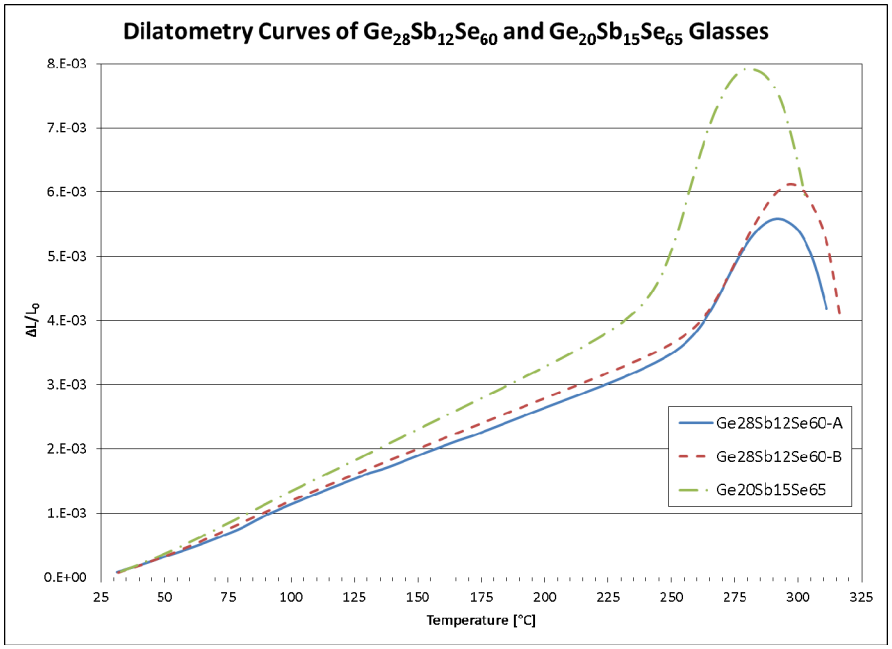

Figure 9 – Dilatometry curves of various glass samples.

Looking at the figure, one can see that the $Ge_{28}Sb_{12}Se_{60}$ glasses have higher T_g's and T_d's than the $Ge_{20}Sb_{15}Se_{65}$ glass, as expected. The figure also shows that the CTE of the $Ge_{20}Sb_{15}Se_{65}$ glass increases more significantly after the T_g than the $Ge_{28}Sb_{12}Se_{60}$ glasses. This is seen in the more dramatic change in the slope of the curve. The values of the properties determined from Figure 6 are summarized in Table 2 below, along with reported values for equivalent glasses. The temperature ranges of the CTE values of IG5 and AMTIR-3 were not specified.

Table 2: Properties determined from dilatometry measurements on various glasses

Sample	CTE (25-100°C) [/°C]	$T_{g(dil)}$ [°C]	T_d [°C]
$Ge_{28}Sb_{12}Se_{60}$-A	14.9 x 10^{-6}	257	291.8
$Ge_{28}Sb_{12}Se_{60}$-B #1	15.8 x 10^{-6}	261	297.4
*IG5**	*14 x 10^{-6}*	-	-
*AMTIR-3**	*14 x 10^{-6}*	*278*	*295*
$Ge_{20}Sb_{15}Se_{65}$ #1	17.9 x 10^{-6}	244	280.4
*GASIR2**	*16 x 10^{-6} (27°C)*	-	-

For all three of the glass boules tested, the CTE was found to be higher than reported values of equivalent glasses. However, other studies [5] have shown $Ge_{28}Sb_{12}Se_{60}$ to have a CTE of 15 x 10^{-6}/°C even though the reported value for

IG5 and AMTIR-3 is 14 x 10^{-6}/°C. In PGM, the CTE of the mold material must be similar to that of the glass. Changes in the CTE of the glass can affect the residual stress in the lens as well as its shape. The CTE is also important for applications where the lens would be subjected to large temperature variations. A higher than expected CTE could affect the performance of the lens over the temperature range.

The T_g values from dilatometry are around 30°C lower than those from DSC measurements. This is due in part to a slower heating rate used for dilatometry as well as differences in the method for determining the T_g. In dilatometry, the T_g is defined as the temperature where the CTE changes while the T_g is defined by changes in the heat capacity for DSC measurements. Since molding is performed at temperatures well above the T_d, small variations in this property should not affect the PGM process.

3.4 Density

The density of glass discs from various boules of glass was determined using Archimedes' method. The results are shown in Figure 10. Error bars are within the size of the data points.

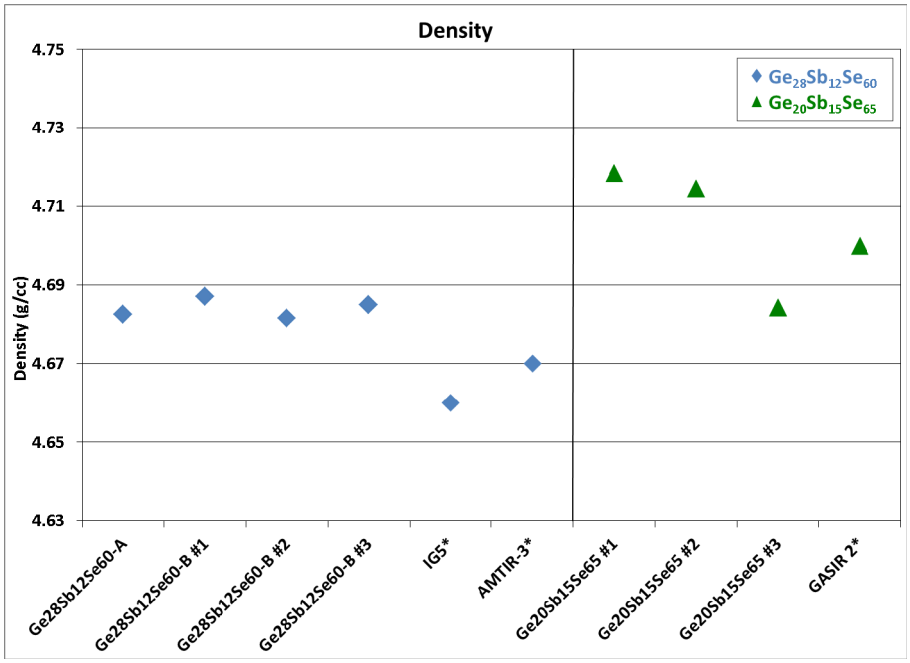

Figure 10 – Comparison of density values of various glass boules. *Indicates values from published data sheets.

As was seen with the other results discussed so far, there is very little variation between the $Ge_{28}Sb_{12}Se_{60}$ samples. This indicates that the process for making the glass is very consistent and the properties are predictable.

Again, there is some variation seen between different boules of the $Ge_{20}Sb_{15}Se_{65}$ glass. Density can be expected to be related to the density of each element making up the material and the amount of each of those elements. As seen in the figure, the sample from $Ge_{20}Sb_{15}Se_{65}$ #3 has a somewhat lower density than that of the other two $Ge_{20}Sb_{15}Se_{65}$ samples. It's possible to explain this based on the compositional analysis discussed in section 3.1. $Ge_{20}Sb_{15}Se_{65}$ #3 was found to have lower antimony content and higher selenium content than the other 2 samples. Since selenium has the lowest density (4.28 g/cc) and antimony has the highest density (6.697 g/cc) of the 3 elements making up the glass, it is understandable that sample $Ge_{20}Sb_{15}Se_{65}$ #3 has a lower density.

Variations in density are important because they could indicate variations in other properties of the glass. This is a quick, simple, and inexpensive test that can give some insight into deviations from the desired material properties.

3.5 Hardness

Nano indentation measurements were made on each sample and the Vickers hardness (H_V) and Young's modulus (E) values were calculated. Five measurements were made on each sample and the results were averaged. The average values for each property are shown below in Figures 11 and 12.

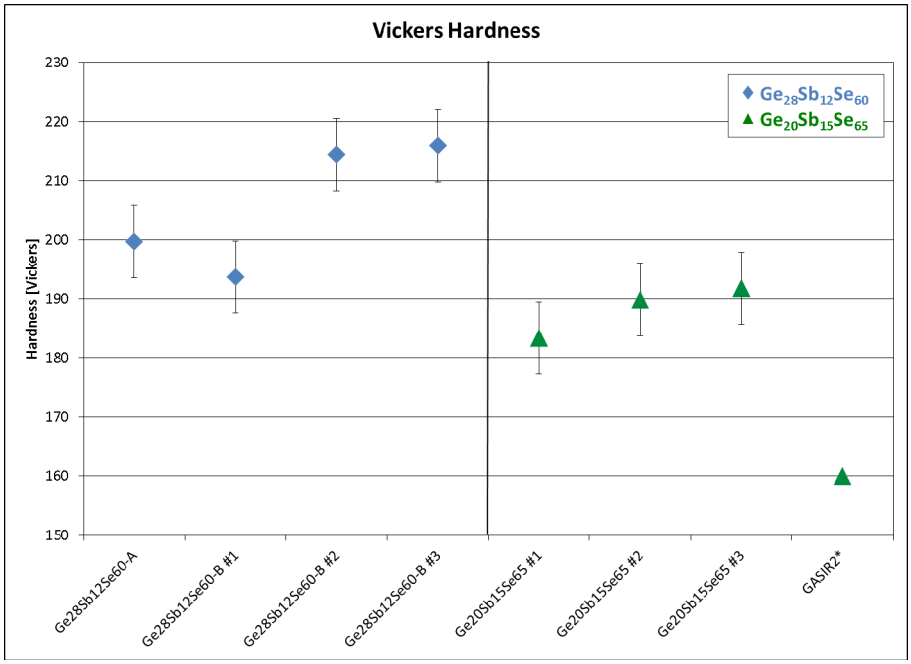

Figure 11 – Hardness of $Ge_{28}Sb_{12}Se_{60}$ and $Ge_{20}Sb_{15}Se_{65}$ glasses. *Indicates values from published data sheets.

Hardness is the only property measured in which the $Ge_{28}Sb_{12}Se_{60}$-B glass boules had more variability than the $Ge_{20}Sb_{15}Se_{65}$ boules. Differences in surface roughness can have a small effect on the hardness measurements, so this could account for some of the variation seen. However, all of these glasses have relatively low hardness values and lenses molded from these materials must have a hard coating applied. For this reason, small variations in hardness are not expected to affect the PGM process, although large variations could indicate a problem with the material and could also affect the process of polishing preforms.

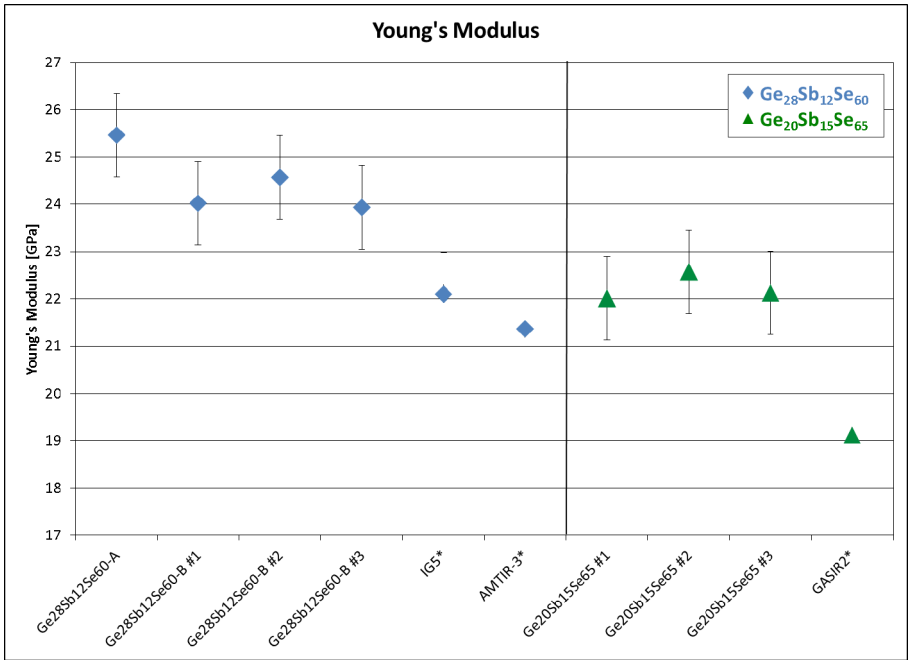

Figure 12 – Young's Modulus of $Ge_{28}Sb_{12}Se_{60}$ and $Ge_{20}Sb_{15}Se_{65}$ glasses. *Indicates values from published data sheets.

The values of E are all within error for both glass compositions, so it can be concluded that there is no significant variation in E from boule to boule or manufacturer to manufacturer. With both compositions, the experimental values of E are higher than the reported values for equivalent glasses. The rate at which the load is applied can affect the value of E, which is determined from the slope of the linear section of the stress-strain curve. Since this rate is not reported on the data sheets for IG5, AMTIR-3, or GASIR2, it could be a source of the differences.

Young's Modulus indicates how much a material deforms under a load. Since a load is applied during the molding process, these values could be important in determining the molding parameters. The low variation between samples indicates good consistency for PGM.

3.6 Fourier Transform Infrared Spectroscopy (FTIR)

Transmission FTIR spectra were measured for each sample in order to determine the spectral range and to compare impurity levels in the various glass boules. Differences in surface quality between samples prevented the determination of the absolute percent transmission. The spectra were normalized for easier comparison between them. The results for $Ge_{28}Sb_{12}Se_{60}$-A and the three $Ge_{28}Sb_{12}Se_{60}$-B boules of glass are shown in Figure 12 below.

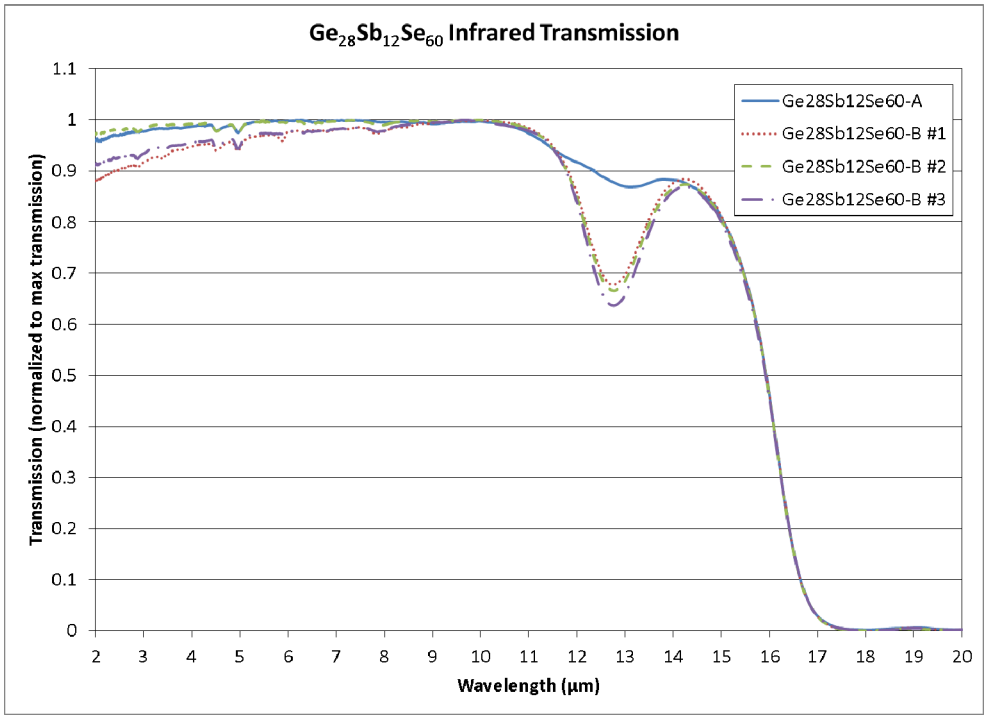

Figure 12 – Normalized infrared transmission spectra of various boules of $Ge_{28}Sb_{12}Se_{60}$ glass.

The variations in the overall transmission are most likely due to differences in the surface quality of the polished discs. The absorption band located at approximately 12.5 μm is due to oxide impurities in the form of Ge-O bonds. [6] All three $Ge_{28}Sb_{12}Se_{60}$-B boules have similar levels of oxide impurity based on the size of the absorption bands. The $Ge_{28}Sb_{12}Se_{60}$-A glass has a much lower oxide content, indicating that it has undergone purification at some point in the process while the $Ge_{28}Sb_{12}Se_{60}$-B glass has not.

The normalized IR transmission spectra of the three $Ge_{20}Sb_{15}Se_{65}$ boules of glass are shown below in Figure 13.

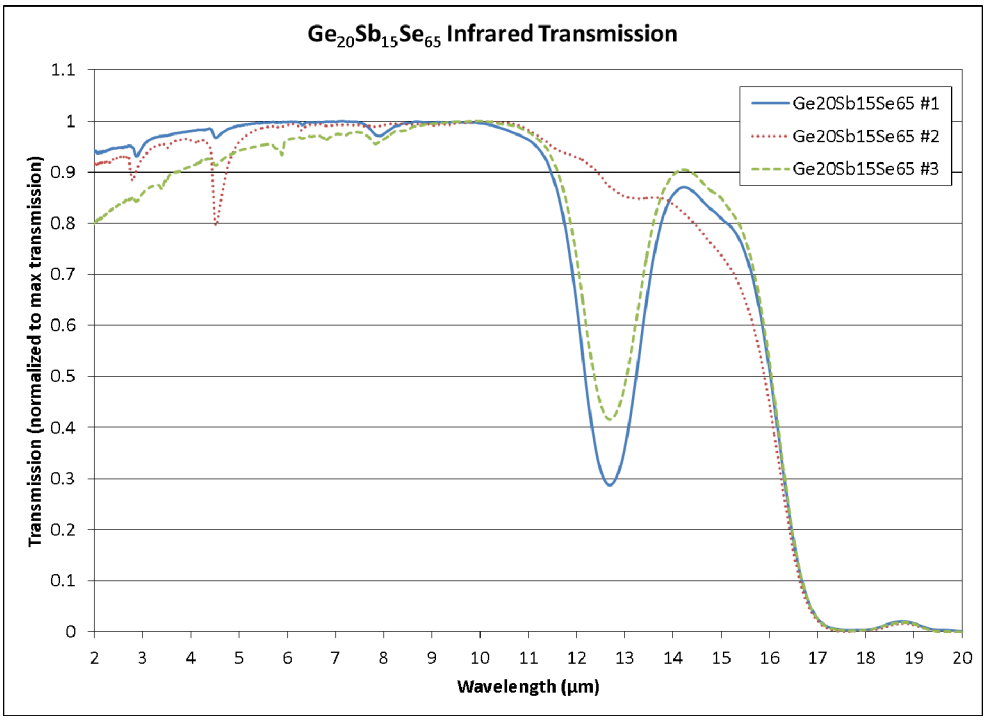

Figure 13 – Infrared transmission spectra of various boules of $Ge_{20}Sb_{15}Se_{65}$ glass.

The variations in overall transmission are again most likely due to differences in surface quality of the samples as well as slight differences in sample thickness. As seen in the figure, there is much more variation in the spectra of the $Ge_{20}Sb_{15}Se_{65}$ glasses than $Ge_{28}Sb_{12}Se_{60}$-B. This is not unexpected due to variations in other properties discussed in the previous sections. Looking at the absorption band at 12.5 µm, which is due to Ge-O impurities [6], boule #1 has the highest oxide impurity level while boule #3 also has a high impurity level. Interestingly, boule #2 has a very low oxide content. However, its overall transmission starts to reduce sooner than that of the other two boules. There is also a new impurity seen, Se-H, which appears as the absorptions at 4.5 µm. [6] The small absorption at 2.7 µm may be due to OH^- impurities, most likely in the form of Ge-OH, and is seen for boule #1 and boule #2. [6] It appears that the manufacturer of $Ge_{20}Sb_{15}Se_{65}$ may have a purification process but it is not consistent.

For thermal imaging applications, the spectral range used is 8-14 µm. Boules #1 and #3 give very low transmission values in the 12-14 µm range which would negatively impact performance.

3.7 Refractive Index

The refractive index of a prism made from $Ge_{28}Sb_{12}Se_{60}$-B was measured from 1.5-14 µm and compared to reported values from the manufacturer data sheet as well as Schott's IG5. The measurements were made at 20°C in air. The dispersion curves are shown below in Figure 14.

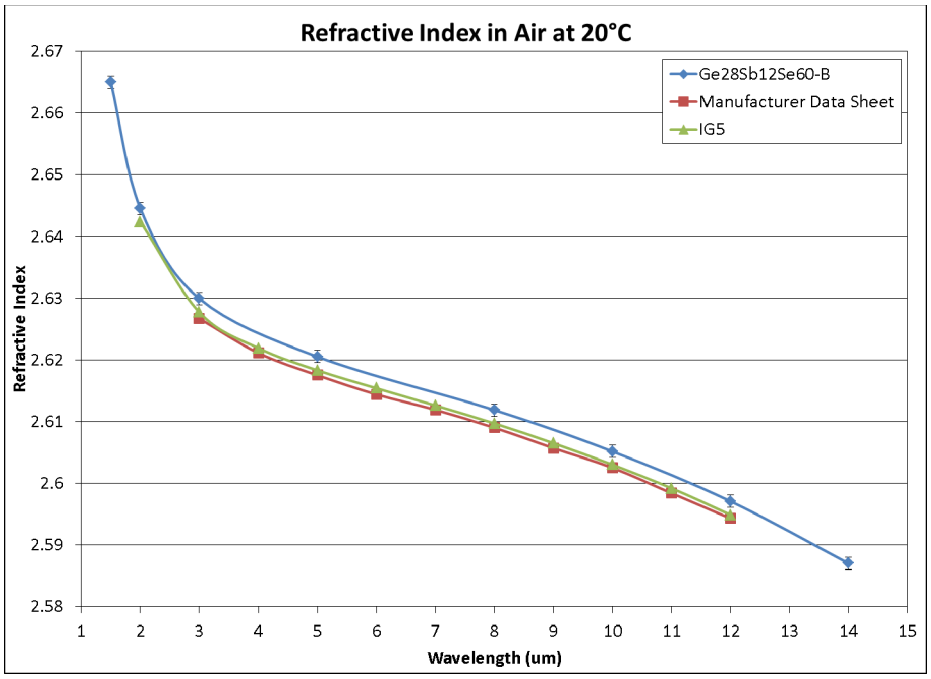

Figure 14 – Refractive index of $Ge_{28}Sb_{12}Se_{60}$-B

As seen in the figure, the measured index is slightly higher than reported values at all wavelengths. However the difference is relatively small and the index of glass decreases after molding. The index drop after molding is typically larger than the differences seen here, so it would most likely not affect the lens quality.

Another important property is dn/dT. This is important because the lenses may be used at different temperatures depending on the application. For $Ge_{28}Sb_{12}Se_{60}$-B, the index was measured from -40°C to 80°C at 1.5, 2, 3, 5, 8, 10, 12, and 14 µm. Then the dn/dT was calculated and the results are shown in Figure 15 and compared to values for IG5 (measured from -50°C to 75°C).

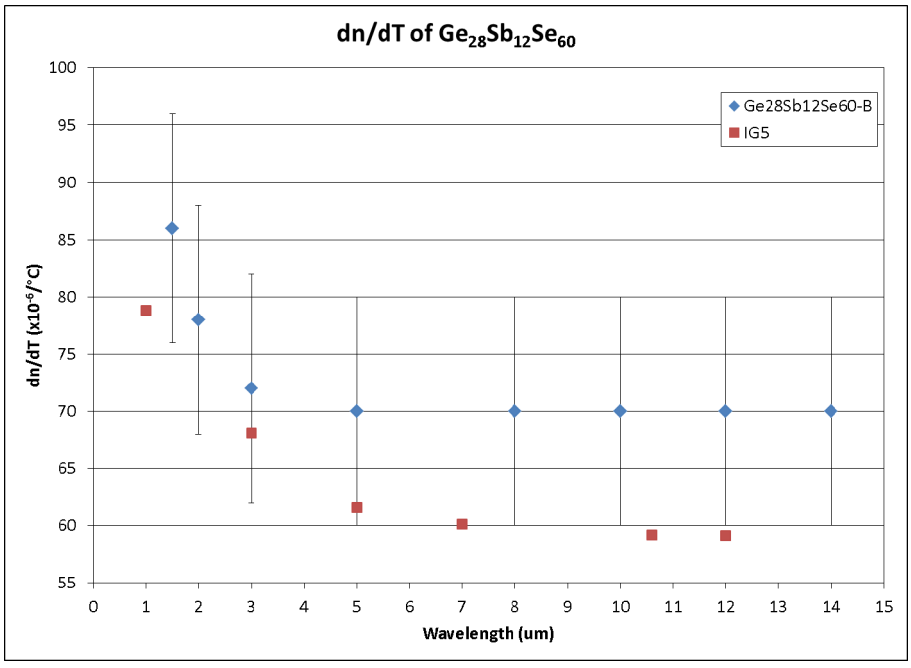

Figure 15 – Change in refractive index with temperature for $Ge_{28}Sb_{12}Se_{60}$ at various wavelengths

Although the dn/dT values measured for $Ge_{28}Sb_{12}Se_{60}$-B are higher than those reported for IG5, they are similar and the differences are most likely within the error of the measurement if the error bars were known for IG5. Compared to crystalline germanium, this chalcogenide glass is clearly superior with regards to dn/dT. Crystalline germanium has a dn/dT that is on the order of 4 x 10^{-4}/K near room temperature. [7]

4. CONCLUSIONS

The purpose of this study was to compare material performance and variability of different glass manufacturers. Based on the results, it is clear that there can be significant differences between manufacturers. Although of slightly different compositions, the variability of the properties of $Ge_{28}Sb_{12}Se_{60}$-B and $Ge_{20}Sb_{15}Se_{65}$ glass boules can still be compared. While the properties of the $Ge_{28}Sb_{12}Se_{60}$-B glass were very consistent from boule to boule, there were significant variations seen between different $Ge_{20}Sb_{15}Se_{65}$ boules of glass. As far as IR transmission, 2 of the $Ge_{20}Sb_{15}Se_{65}$ boules had very low performance due to oxide impurities that caused absorption in the 12-14 μm region. While small variations in some of the other properties do not have a substantial effect on the PGM process, IR transmission is very important for the final lens specifications. It is essential to evaluate new manufacturers to be sure the glass has high performance and that there is little variation between boules. Despite the limited data set, indications for high volume production are very good for $Ge_{28}Sb_{12}Se_{60}$ from multiple manufacturers.

The work presented here is the beginning of an ongoing project to evaluate chalcogenide glasses for use in precision glass molding. Future work will include completing the index measurements on all samples compared in this paper, as well as characterizing glass from additional manufacturers and compositions.

ACKNOWLEDGEMENTS

The authors of this paper would like to thank the Infrared Development team at LightPath Technologies for their contributions to this paper. All figures courtesy of LightPath Technologies Inc.

REFERENCES

[1] Bacchus, J.M., “Using new optical materials and DOE in low-cost lenses for uncooled IR cameras” in *Optical Design and Engineering*, edited by Philip J. Rogers, Rolf Wartmann, Proceedings of SPIE Vol. 5249 (SPIE Bellingham, WA, 2004)

[2] Cogburn, G., Mertus, L., Symmons, A., "Molding aspheric lenses for low-cost production versus diamond turned lenses" in *Infrared Technology and Applications XXXVI*, edited by Bjørn F. Andresen, Gabor F. Fulop, Paul R. Norton, Proceedings of SPIE Vol. 7660 (SPIE, Bellingham, WA 2010) 766020.

[3] Schaub, M., Schwiegerling, J., Fest, E., Symmons, A., Shepard, R.H., [Molded Optics: Design and Manufacture], CRC Press, Taylor and Francis Group, London, Chapter 5: Molded Optics, 165-200 (2011)

[4] Foreman, J., Sauerbrunn S.R., Marcozzi, C.L., “Exploring the sensitivity of thermal analysis techniques to the glass transition” in *TA Instruments: Thermal Analysis & Rheology*.

[5] Guery, G., “Influence of iso-structural substitutions on properties of Ge(As,Sb)(S,Se) glasses,” Master’s Thesis, Clemson University (2010).

[6] Kokorina, V.F., *Glasses for Infrared Optics*, CRC Press, Inc. (1996).

[7] Frey, B.J., Leviton D.B., Madison, T.J., “Temperature-dependent refractive index of silicon and germanium,” Proceedings of SPIE Vol. 6273 (SPIE, Orlando, FL 2006) 62732J.